Infection, Genetics and Evolution 69 (2019) 216–223

Contents lists available at ScienceDirect

Infection, Genetics and Evolution

journal homepage: www.elsevier.com/locate/meegid

Malaria infection rates in *Anopheles albimanus* (Diptera: Culicidae) at Ipetí-Guna, a village within a region targeted for malaria elimination in Panamá

Chystrie A. Rigg[a,1], Lisbeth Amarilis Hurtado[b,1], José E. Calzada[a,1], Luis Fernando Chaves[c,*]

[a] Departamento de Investigación en Parasitología, Instituto Conmemorativo Gorgas de Estudios de la Salud, Apartado 0816-02593, República de Panamá
[b] Departamento de Análisis Epidemiológico y Bioestadísticas, Instituto Conmemorativo Gorgas de Estudios de la Salud, Apartado 0816-02593, República de Panamá
[c] Instituto Costarricense de Investigación y Enseñanza en Nutrición y Salud (INCIENSA), Apartado 4-2250, Tres Ríos, Cartago, Costa Rica

ARTICLE INFO

Keywords:
Plasmodium vivax
Nested PCR
Mosquito ecology
Entomologic inoculation rate
Time series models

ABSTRACT

The Panamá Canal construction encompassed one of the first examples of malaria elimination. Nevertheless, malaria has uninterruptedly persisted in Native American populations living within a few kilometers of the Panamá Canal. Here, we present results from a monthly longitudinal study (May 2016 to March 2018), whose goal was to quantitatively describe seasonal patterns of *Plasmodium* spp. infection in *Anopheles albimanus* Wiedemann, and its association with environmental covariates, at Ipetí-Guna, a village within a region targeted for malaria elimination in Panamá. To detect *Plasmodium* spp. infections we employed a standard nested PCR on DNA extracts from mosquito pools of varying size, which were then used to estimate monthly infection rates using a maximum likelihood method. The infection rate estimates (IR) were analyzed using time series analysis methods to study their association with changes in rainfall, temperature, NDVI (a satellite derived vegetation index), malaria cases and human biting rates (HBR). We found that mosquitoes were infected by *Plasmodium vivax* mainly from September to December, reaching a peak in December. Time series modeling showed malaria IR in *An albimanus* increased, simultaneously with HBR, and IR in the previous month. These results suggest that elimination interventions, such as mass drug administration, are likely to be more effective if deployed from the middle to the end of the dry season (March and April at Ipetí-Guna), when the likelihood of malaria infection in mosquitoes is very low and when curtailing human infections driving infections in mosquitoes can reduce malaria transmission, and increase the chance for elimination.

1. Introduction

The study of malaria vectors in Panamá has a long history dating back to the construction of the Panamá Canal (Jennings, 1912; Zetek, 1915), where knowledge about mosquito ecology and behavior proved key to successfully building the Panamá Canal (Gorgas, 1914). Nevertheless, malaria is still a major vector-borne disease in Panamá, with around 900 annual cases according to recent estimates (WHO, 2018), most cases concentrated on indigenous populations (Calzada et al., 2015; Hurtado et al., 2014; Obaldia, 2015; Obaldia et al., 2015), a historical pattern from the time of the Panamá Canal construction (Kendall, 1906a, 1906b). However, malaria elimination is a major health priority in the country (Calzada et al., 2015) and regionally in all Meso-America (Herrera et al., 2015; Herrera et al., 2012).

From about a century ago, it was recognized that *Anopheles albimanus* was the main malaria vector in Panamá (Rozeboom, 1938; Zetek, 1915), a species nowadays known to be widely distributed across Panamá (Loaiza et al., 2008; Torres et al., 2017). Ecological studies have shown that *An. albimanus* thrives at relatively hotter temperatures than commonly co-occurring anopheline mosquito species (Pinault and Hunter, 2012), and it is associated with abundant vegetation as both larvae and adults (Rejmankova et al., 1993; Rejmankova et al., 1992; Rejmankova et al., 1991). *An. albimanus* is also gonotrophically discordant, i.e., bloodmeals do not translate into ovary and egg development, tends to rest (exophilic) and bloodfeed (exophagic) outside houses, and more often feeds on animals other than humans (Breeland, 1972; de Zulueta and Garrett-Jones, 1965; Weathersbee, 1944). Moreover, *An. albimanus* is a vector species that gets easily infected by *Plasmodium* spp. under experimental conditions when bloodfeeding on infected human hosts (Rozeboom, 1942). Our research at Ipetí-Guna, Panamá has shown that *An. albimanus* larvae have three month period abundance cycles, which are sensitive to temperature changes, with

* Corresponding author.
E-mail address: lfchavs@gmail.com (L.F. Chaves).
[1] Contributed equally.

https://doi.org/10.1016/j.meegid.2019.02.003
Received 29 November 2018; Received in revised form 23 December 2018; Accepted 2 February 2019
Available online 04 February 2019

5 months of lag, while adult abundance was correlated with the normalized difference vegetation index (NDVI), with a three months lag (Hurtado et al., 2018b), an association that might partially explain the sensitivity to meteorological fluctuations we have also observed in malaria transmission in the region (Hurtado et al., 2014). However, little is known about the seasonality of malaria infections of *An. albimanus* in Panamá. This information is extremely important, as it could help to optimize the timing of interventions that could help eliminate malaria from Panamá. For example, based on abundance patterns (Hurtado et al., 2018b), the dry season from January to April seems ideal for the deployment of a mass drug administration, MDA, designed to eliminate parasites from the human population, since the likelihood of further infections associated with mosquitoes is minimal (Kaneko, 2010). Nevertheless, it is not clear when during the dry season would be best to implement a MDA, considering the impacts that curtailing human infections might have on furtherly driving down entomological transmission indices (Kaneko et al., 2000), an aspect that has not been explicitly explored by mathematical models of malaria transmission (Brady et al., 2017), which nevertheless have suggested that IR increases with mosquito abundance (Brady et al., 2017; Smith et al., 2010). Based on these observations we have the hypothesis that malaria infection rates in mosquitoes increase with mosquito population size and with short term changes in human malaria infection. We also expect that temperature does not play a major role in limiting the seasonality of infections, provided temperature fluctuations at Ipetí-Guna (Hurtado et al., 2018b) are within the optimal range for *Plasmodium* spp. parasite development (Chaves, 2017). To test these hypotheses, we conducted a two-year longitudinal study, from May 2016 to March 2018, where we collected adult anopheline mosquitoes monthly and studied *Plasmodium* spp. infection in mosquito pools with varying size using a standard nested PCR technique (Snounou et al., 1993) that allows the identification of malaria infections at the species level.

2. Materials and methods

2.1. Study site, environmental covariates and mosquito collections

This study was done in Ipetí-Guna (8°58′12″ N, 78°30′36″ W) a village located in Comarca Madungandí, Distrito de Chepo, Panamá Province, República de Panamá (Fig. 1A). At the study site housing conditions are very precarious, and almost 100% of the houses have ventilation eaves which favor the entrance of *Anopheles* spp. (Hurtado et al., 2014; Kendall, 1906a, 1906b). During the study period 28 *Plasmodium vivax* malaria human infections were detected via blood slide examination of febrile cases attending the health post at Puente Bayano, all infections detected among members of the indigenous Guna population residing at the study area. During the study period the *P. vivax* infections did not show a clear seasonal pattern, instead scattered cases occurred through the year (Fig. 1B).

Weather variables included temperature (Fig. 1C) and rainfall (Fig. 1D), which came from gridded databases. Both weather variables have a strong seasonality, where temperatures are hotter during the dry season, especially from February to June (Fig. 1C), while rainfall is mostly absent during the dry season from January to April (Fig. 1D). Temperature came from a cell with a 0.5° spatial resolution from the NOAA Global Historical Climatology Network version 2 and the Climate Anomaly Monitoring System (GHCN_CAMS 2 m model) (NOAA, 2018a). Rainfall had a 0.25° spatial resolution and came from the NOAA CPC Morphing Technique ("CMORPH") database (NOAA, 2018b). Data was extracted from both databases using the tools available for weather data extraction at the KNMI website (KNMI, 2018). We also employed data for the Normalized Difference Vegetation Index, NDVI (Fig. 1E), a proxy for vegetation growth (Pettorelli et al., 2005). Monthly satellite based (MOD13Q1) NDVI products with a 250-m resolution (Didan, 2015) were used in the analysis. The NDVI products are courtesy of the NASA Land Processes Distributed Active Archive Center (LPDAAC), USGS/Earth Resources Observation and Science (EROS) Center (Sioux Falls, South Dakota). NDVI products were downloaded from LPDAAC server (NASALPDAAC, 2018) using the package *MODIStsp* for the software R (Busetto and Ranghetti, 2016), and values extracted for the cell containing our sampling site using the package *raster* for R (Brunsdon and Comber, 2015). Overall, NDVI does not have a strong seasonality at the study site, but values tend to be smaller during the dry season from January to April (Fig. 1E).

Adult mosquitoes were collected by human landing catch, HLC, at a peridomicile cluster (Fig. 1A) chosen by the nearby abundance of positive anopheline larval habitats and distances between 5 and 10 m to the nearest inhabited housing units (Hurtado et al., 2018b). HLC was chosen because it is a highly sensitive sampling method for anopheline mosquito malaria vectors (Rubio-Palis and Curtis, 1992a,b; Rubio-Palis et al., 2012). As previously described by Hurtado et al. (2018b) monthly HLC collections were made over three consecutive nights by three trained collectors that minimized bias in the abundance estimates by switching their positions (Rubio-Palis and Curtis, 1992a,b). Collections were made from 18:00 h to 21:00 h based on reports that *An. albimanus* has an unimodal peak of biting activity shortly after dusk (Breeland, 1972; Hobbs et al., 1986; Zimmerman, 1992). HLC collections were done from May 2016 to March 2018. With mosquito counts from the HLC we estimated the Human Biting Rate (HBR), which is defined as the number of mosquitoes collected by one person over 12 h (Beier et al., 1994; Macdonald, 1952; Rubio-Palis et al., 1992), which in the case of this study was obtained by multiplying by 0.444 the total monthly number of mosquitoes collected by HLC, provided HLC was performed during 9 h per month, by 3 people. Malaria infection risk was minimized by following World Health Organization (WHO) biosecurity guidelines (WHO, 1993). Mosquitoes were identified using an illustrated taxonomic key for anophelines of Meso-America (Wilkerson et al., 1990) and the Reference Collection at the Gorgas Institute.

2.2. DNA extraction and malaria diagnostics

DNA was extracted from adult female mosquito pools of varying size (between 1 and 7 individuals). Briefly, pools were macerated in 180 μl of PBS 1× and furtherly processed according to the protocol described by the DNeasy Blood and Tissues Kit DNA extraction kit (QIAGEN, Hilden, Germany). The extracted DNA was processed by a nested PCR to amplify species-specific sequences of the small sub-unit ribosomal ribonucleic acid (ssrRNA) genes of *P. vivax*, *P. falciparum*, using a slightly modified protocol based on Snounou et al. (1993).

Briefly, the protocol consists of two PCR reactions. In the first PCR reaction a region common to all *Plasmodium* spp. is amplified using the following primers: rPLU6 5′-TTA AAA TTG TTG CAG TTA AAA CG-3'and rPLU5 5′-CCT GTT GTT GCC TTA AAC TTC-3′; under the following conditions: 2 min at 94 °C for an initial DNA denaturation, 25 cycles as follows: denaturation 94 °C for 1 min, hybridization at 58 °C for 2 min, extension ay 72 °C for 2 min, and a final extension at 72 °C for 2 min.

Amplified samples were then subject to a second PCR with primers specific for *Plasmodium falciparum* (rFAL1 5′-TTA AAC TGG TTT GGG AAA ACC AAA TAT ATT-3'and rFAL2 5-'ACA CAA TGA ACT CAA TCA TGA CTA CCC GTC-3′), and for *P. vivax* (rVIV1 5′-CGC TTC TAG CTT AAT CCA CAT AAC TGA TAC-3'and rVIV2 5′-ACT TCC AAG CCG AAG CAA AGA AAG TCC TTA-3′). Conditions for this second reaction were as follows: 2 min at 94 °C for an initial DNA denaturation, 35 cycles as follows: denaturation 94 °C for 30 s, hybridization at 65 °C for 1 min, extension ay 72 °C for 1 min, and a final extension at 72 °C for 4 min (Snounou et al., 1993). As positive controls we used the *P. vivax* SAL1 and *P. falciparum* 3D7 reference strains. We employed a negative control including all reagents but no DNA. Amplified products were analyzed with an 1.5% agarose gel electrophoresis using a TBE 0.5× buffer. Ethidium bromide was used for DNA staining, and agarose gels were examined using an ultraviolet transilluminator (UVP BioDoc-It System).

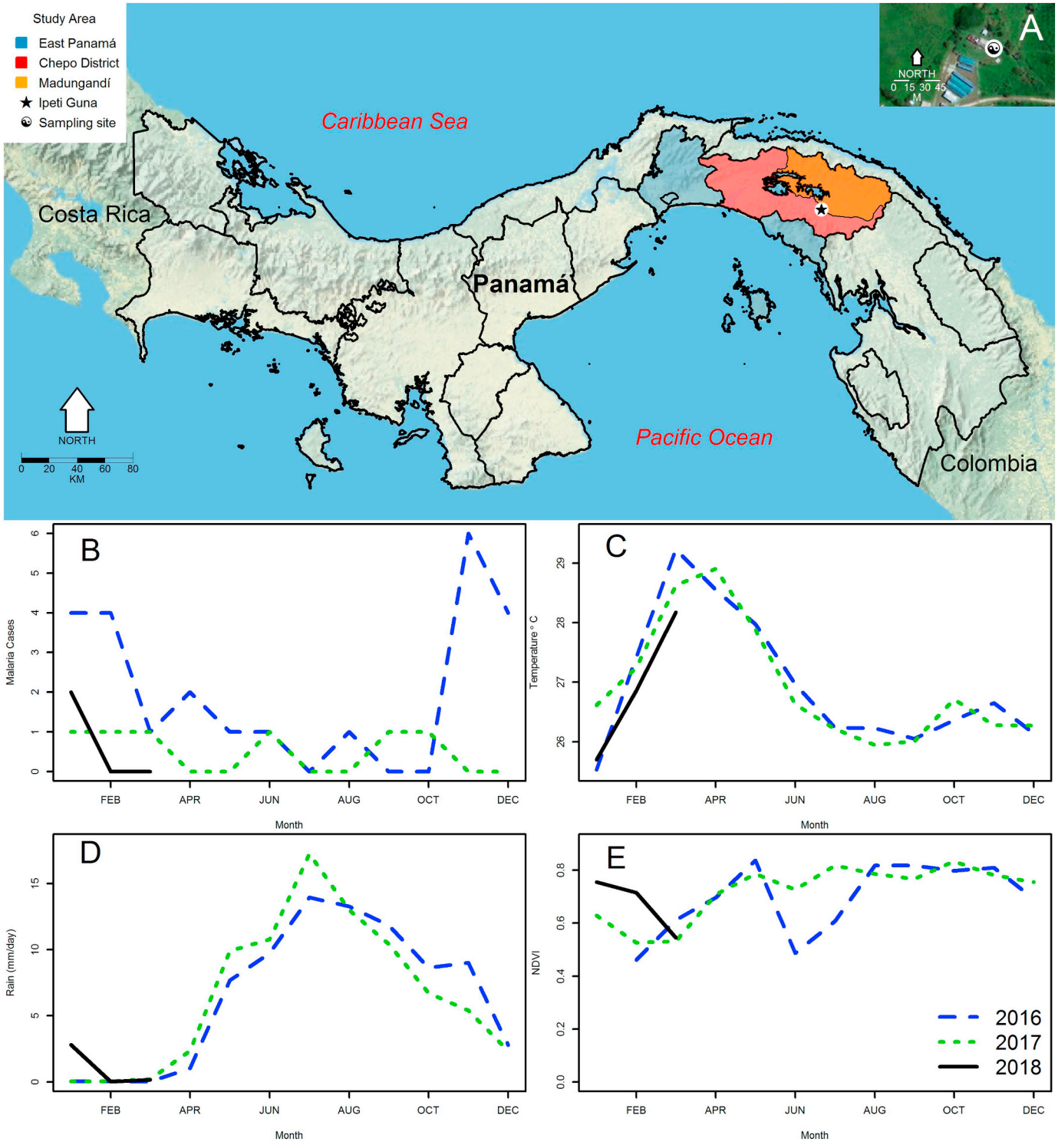

Fig. 1. Study site and time series for malaria cases and environmental variables at Ipetí-Guna (A) Map of Panamá showing the study location at Ipeti Guna. In the map, East Panamá province is highlighted, including Chepo District and the Comarca Guna de Madugandí. In the upper right corner an aerial image, courtesy of Google, shows the location where adult mosquitoes were collected. (B) Malaria cases from Ipetí-Guna (from January 2016 to March 2018), (C) Rainfall (from January 2016 to March 2018), (D) Temperature (from January 2016 to March 2018), (E) NDVI (from January 2016 to March 2018). In panels B to E the year is indicated by line type (see inset legend of panel E).

2.3. Statistical analysis

We estimated monthly malaria infection rates using data from all *An. albimanus* pools collected in the same month. Assuming the nested malaria PCR had a sensitivity near 1, we used a maximum likelihood estimation method for infection rate estimation based on pools with unequal size (Speybroeck et al., 2012). In this method infections rates are estimated with a complimentary log-log link generalized linear model (Farrington, 1992) and confidence intervals are estimated by inverting a likelihood ratio test (Speybroeck et al., 2012). Monthly malaria infection rate estimates, IR, were then used to build a time series for the studied period. The IR time series was then studied using a

standard procedure for time series analysis (Chaves, 2016; Chaves et al., 2015; Chaves and Moji, 2018). This standard method consists in estimating the auto-correlation function (ACF) and Partial ACF of a focal time series, in this case the monthly malaria infection rate, which is then used to fit a null model that is used to pre-whiten the covariates time series. Pre-whitened environmental covariates included: Rainfall, Temperature, NDVI (250 m resolution) and we also pre-whitened time series for the human biting rate estimates and number of malaria cases. The pre-whitened time series and the residuals of the null model were then used to estimate cross-correlation functions which were used to assess the correlation, at different time lags, between all the different covariates and mosquito infection rates (Shumway and Stoffer, 2011). Further details about the methods for time series analysis have been presented elsewhere (Hoshi et al., 2014; Hoshi et al., 2017; Hurtado et al., 2018b). Finally, with the average daily HBR and assuming that infection rates (IR) estimated with the PCR results were representative of sporozoite infections, we estimated the daily entomological inoculation as follows:

$$EIR = HBR^{*}IR \quad (1)$$

And the annual entomological inoculation rate (AEIR) by multiplying the EIR from eq. (1) by 365.

2.4. Ethical statement

This study was performed by the Instituto Conmemorativo Gorgas de Estudios de la Salud (ICGES) as part of the national surveillance effort to eliminate malaria from Panamá. The latter is a concerted effort with consent, approval and participation of authorities, professional and technical personnel from Ministerio de Salud de Panamá (MINSA) and ICGES. Ethical and technical considerations to use human landing catch as the sampling method, by members of MINSA and the ICGES as part of their job responsibilities, to monitor *Anopheles* spp. populations vectors of malaria are presented in the national malaria norm (Ministerio de Salud de Panamá, 2011).

3. Results

We made 322 pools out of 1584 *Anopheles* spp. female adult mosquitoes collected by HLC. Most pools were from *An. albimanus* ($n = 1567$, 315 pools, 69 positive). The seven remaining pools were for other species, which included: *Anopheles apicimacula* Dyar & Knab (n = 1, 1 pool), *Anopheles punctipennis* (Say) (n = 1, 1 pool) and *Anopheles punctimacula* Dyar & Knab (n = 15, 5 pools). All the pools for species different from *An. albimanus* had no *Plasmodium* spp. infections. All of the *An. albimanus* positive pools were positive to *P. vivax* (Fig. 2).

During the study period *An. albimanus* monthly (mean ± SD) $\widehat{HBR}$ was 30.92 ± 41.42 bites/person/night. Mosquitoes were, in general, present from June to January (Fig. 3A), with a low HBR during March in 2018, following unusual rain that occurred during the dry season of Panamá, specifically in February 2018 (Fig. 1D). For each of the studied seasons, there was an abundance peak in September, which follows a peak in the rainfall that occurs in July (Fig. 1D). The peak of *P. vivax* infections occurred in December, and the temporal span of malaria infections in mosquitoes was shorter than the active season for adult *An. albimanus* mosquitoes, spanning only from September to December (Fig. 3B). During the study period the average monthly *P. vivax* infection rate ($\widehat{IR}$), expressed as a %, in *An. albimanus* (mean ± SD) was 1.80 ± 3.24. Interestingly in March 2018, the few mosquitoes collected, which were 15 in total and divided in 3 pools, with 1 positive pool, explaining the relatively high infection rate observed in that month, which was around 8% (Fig. 3B). Based on the average monthly $\widehat{HBR}$ and $\widehat{IR}$ the daily entonomologic inoculation rate ($\widehat{EIR}$) was (mean ± SD) 0.556 ± 1.755 infective bites/person/night, and the annual EIR ($\widehat{AEIR}$) was 202.777 ± 640.575 infective bites/person/year.

The autocorrelation pattern of the *P. vivax* infection rates in adult *An. albimanus* mosquitoes (*IR*) indicated the time series was a 1st order autoregressive time series, i.e., IR was significantly associated with itself with one month of lag (Fig. 4A). Based on this information a null autoregressive model was fit, described by the following equation:

$$IR_t = \mu + \rho(IR_{t-1}) + \varepsilon \quad (2)$$

where t indicates time (in months), μ is the mean infection rate during the study period, ρ is an autocorrelation coefficient and $\varepsilon \sim N(0, \sigma^2)$, indicating the error ($\varepsilon$) is an independent, homogenous, and normally distributed variable with mean 0 and variance (σ^2). The model presented in (2) was then used to pre-whiten the environmental variables, which in turn were used to estimate cross-correlation functions with the residuals from the model presented in (2). Results from the cross-correlation functions showed that HBR and IR were significantly ($P < .05$) correlated without a time lag (Fig. 4B), but no significant correlations were observed at any time lag between IR and: malaria cases (Fig. 4C), temperature (Fig. 4D), rainfall (Fig. 4E) and NDVI (Fig. 4F). Based on this information we fitted a model described by the following equation:

$$IR_t = \mu + \rho(IR_{t-1}) + \alpha(HBR_t) + \beta(IR_{t-1})(HBR_t) + \varepsilon \quad (3)$$

where most variables and parameters have the same meaning, and interpretation, that were already presented for Eq. (2). Meanwhile parameter α denotes the impact of HBR on IR and β accounts for the synergistic effect of HBR and IR.

Parameter estimates for the model presented in Eq. (3) are shown in Table 1, which shows the parameter for synergistic impact of abundance and IR ($\widehat{\beta}$) is positive, with a similar pattern for mosquito abundance ($\widehat{\alpha}$), but negative for the autocorrelation parameter ($\widehat{\rho}$). The model presented in Table 1 had an $R^2 = 0.67$, which is relatively high, and the model was statistically significant ($F_{3,18} = 11.98$, $P < .00015$). A graphical representation of the surface generated by the parameter estimates, and its comparison with the observed IRs used to fit the model, is presented in Fig. 5. This figure shows how the IR increased in a nonlinear fashion as both HBR and IR the previous month increased across the study period. Fig. 5 also shows how the positive impact of mosquito abundance and its interaction with the one month lagged IR had a preponderant impact when compared with the negative autocorrelation parameter, thus explaining why no decrease in IR is observed when IR_{t-1} increases in the y axis of Fig. 5.

4. Discussion

Our data showed that *An. albimanus* was the only mosquito species infected by *P. vivax* at the study site, confirming its role as a major malaria vector in Panamá (Loaiza et al., 2008; Rozeboom, 1938; Zetek, 1915). Assuming that infections detected via PCR could be equated with sporozoite infections (Echeverry et al., 2017; Póvoa et al., 2000), the EIR of 0.55/person/night implies that it takes at least two nights to get an infective bite, and that is a value relatively low when compared with worldwide estimates from endemic areas (Smith et al., 2010), especially with what has been reported for *Anopheles gambiae s.l.* Giles in Sub-Saharan Africa (Beier et al., 1999; Beier et al., 1994; Drakeley et al., 2003; Kilama et al., 2014; Patz, 1998). However, EIR and HBR at Ipetí-Guna are extremely high when compared with estimates for *An. albimanus* in other regions where this species is present in the New World. For example, at Guna Yala, in Panamá, HBRs for *An. albimanus* ranged from 10.1 to 15.2 (Calzada et al., 2015), i.e., between 1/3 and 1/2 of what we recorded at Ipetí-Guna. In Colombia *An albimanus* has not been found infected in recent surveys in endemic areas, i.e., EIR is by definition 0, where HBRs, ranged from 1.10 to 3.93 in la Guajira (Herrera-Varela et al., 2014) and from 0.1 to 4.4 in the Pacific región (Naranjo-Díaz et al., 2014). These HBR estimates were lower than what we observed at Ipetí-Guna, which was one order of magnitude higher at 30.92. This difference might be related to the difference in the sampling periods, which in our study was monthly and continuous through the

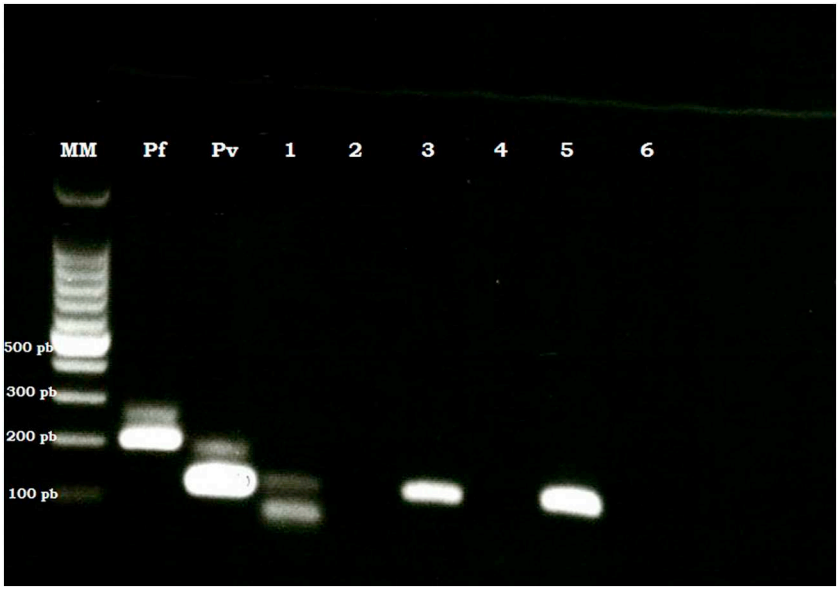

Fig. 2. Nested PCR electrophoresis used to diagnose *Plasmodium* spp. Infection. MM lane shows the 100-bp DNA ladder (Promega), PF is the positive control for *Plasmodium falciparum* (205 bp), PV is the positive control for *Plasmodium vivax* (120 bp), lanes 1 to 5 are samples from adult female *Anopheles albimanus* pools (lanes 1, 3 and 5 are positive, while 2 and 4 are negative), lane 6 is a negative control with a mixture of all reagents without DNA primers.

2 year study period, while in the two studies in Colombia only a few months were sampled (Herrera-Varela et al., 2014; Naranjo-Díaz et al., 2014). The EIR of *An. albimanus* was lower than what has been observed for other dominant malaria vectors in the neotropics, for example, *Anopheles nuneztovari* Gabaldón, *Anopheles albitarsis* Arribazalga and *Anopheles oswaldoi* Peryassu in Venezuela, which ranged from 2.8 to 360, where those high values were mainly due to extremely high HBRs (Rubio-Palis et al., 1992). The HBR of *An. albimanus* at Ipetí-Guna was, however, similar to what has been observed for *An. nuneztovari* in Antioquia, Colombia (Naranjo-Diaz et al., 2013).

Our estimated malaria IR of 1.87% was relatively low when compared with other estimates for *An. albimanus* in Meso-America. For example, based on mosquito dissections and microscopic examination, an IR of 3.70% was reported for a survey made in El Salvador in the 1970's (Warren et al., 1975). Our estimate is significantly higher than the reported range of 0.03 to 0.57% based on sporozoite ELISAs performed in Guatemala (Beach et al., 1992). Here, it is worth highlighting that several factors might underpin these differences, the first one being that the PCR we used detects DNA that does not necessarily belong to sporozoites. However, making such an assumption is probably adequate to still have relatively unbiased malaria infection detection (Echeverry et al., 2017; Póvoa et al., 2000). This is because our PCR is more accurate than using sporozoite ELISAs to detect malaria infections (Póvoa et al., 2000). Related to this was the trade-off between bisecting mosquitoes before performing the PCR (Foley et al., 2012), since, on one hand, our method can detect parasites in both the abdomen (which, when infected, has oocysts, a malaria parasite stage not infective to humans) and salivary glands (where the sporozoites, i.e., the infective malaria forms, are found in mosquitoes), thus likely resulting on a slight overestimation for the EIR, but, on the other hand, bisection can also lead to a potential IR overestimation when cuts are not perfect, or IR underestimation due to DNA degradation and lost during sample preparation (Foley et al., 2012). We think studies like ours could benefit from using more sensitive quantitative PCR methods that can detect *Plasmodium* spp. parasites at lower densities than those detected by the PCR we used (Echeverry et al., 2017; Rockett et al., 2011).

As expected, *Plasmodium* spp. infections in mosquitoes were not directly sensitive to temperature fluctuations at our study site. This result likely reflects that temperature, at Ipetí-Guna (Hurtado et al., 2018b), varies within a range optimal for *Plasmodium* spp. development in anopheline mosquitoes (Chaves, 2017; Hurtado et al., 2014; Patz and Olson, 2006). Nevertheless, our IR time series model found that IRs were positively correlated with HBRs. Our previous results have shown that population dynamics, based on the same human landing catch data used to estimate HBRs in this study, of *An. albimanus* at Ipetí-Guna were associated with vegetation growth, measured through the NDVI

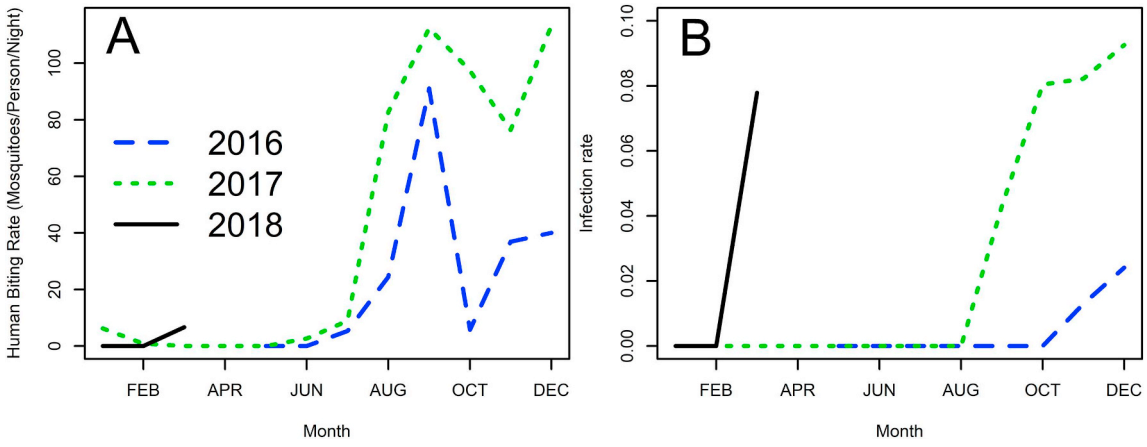

Fig. 3. Monthly Time Series for *Anopheles albimanus* (A) Human Biting Rate (B) *P. vivax* infection rate (presented as a proportion). In both panels the year is indicated by line type (see inset legend of panel A) and data came from *An. albimanus* collected by human landing catch at Ipetí-Guna from May 2016 to March 2018.

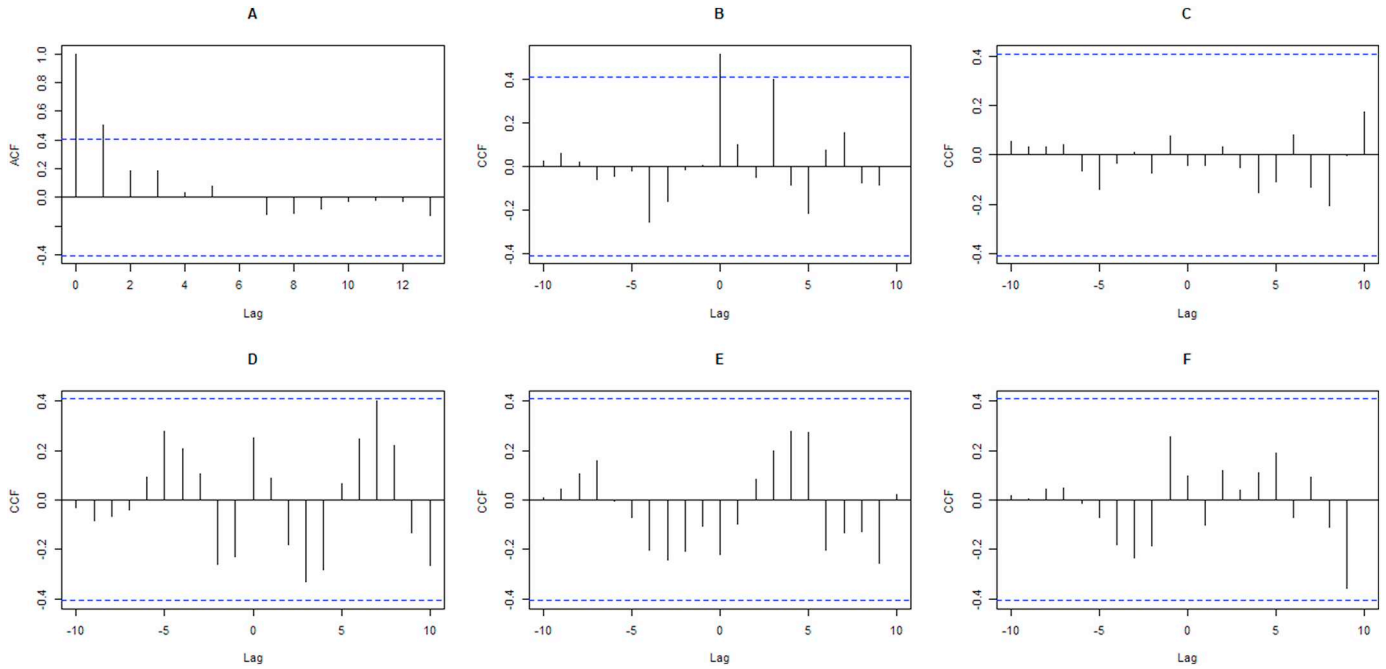

Fig. 4. Correlation analysis (A) Malaria infection rate, IR, auto-correlation function, ACF (B) IR and human biting rate cross-correlation function, CCF (C) IR and malaria cases CCF (D) IR and temperature CCF (E) IR and rainfall CCF (F) IR and Normalized Difference Vegetation Index CCF.

Table 1
Parameter Estimates for the best model explaining monthly *Plasmodium vivax* infection rates (IR) detected by the nested PCR in *Anopheles albimanus* mosquito pools from Ipeti Guna, República de Panamá (2016–2018). HBR indicates the monthly human biting rate, measured as bites/person/night.

Parameter (lag)	Symbol	Estimate	S. E.	*t* value	Pr(> |*t*|)
Intercept	$\hat{\mu}$	0.00507	0.00596	0.851	0.4059
IR (1)	$\hat{\rho}$	−0.0226	0.2228	−0.101	0.9203
An. albimanus HBR (0)	$\hat{\alpha}$	0.000172	0.000137	1.254	0.2259
IR (1) * HBR (0)	$\hat{\beta}$	0.00920	0.00328	2.807	0.0116*
Error SD	$\hat{\sigma}$	0.02052	–	–	–

* Statistically significant (P < .05).

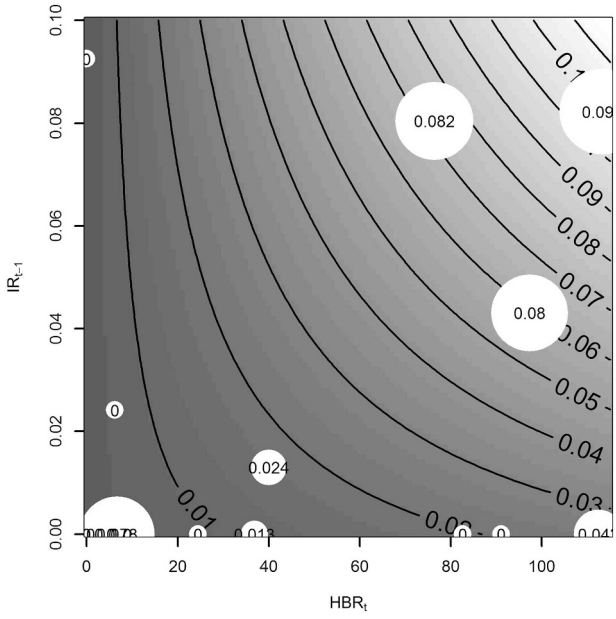

Fig. 5. Surface of predicted *Plasmodium vivax* malaria infection rates (IR) in *Anopheles albimanus* collected by human landing catch at Ipetí-Guna from May 2016 to March 2018. The surface was generated employing the parameters presented in Table 1 and isoclines show the expected values for malaria infection rates at time t (IR$_t$), as function of the infection rates at time t-1 (IR$_{t-1}$) and the *An. albimanus* human biting rate at time t (HBR$_t$). White circles show the observed infection rates, i.e., the monthly maximum likelihood IR estimated from the raw pools.

(Hurtado et al., 2018b). This result suggests that sensitivity of malaria transmission to environmental factors in Panamá (Hurtado et al., 2014; Hurtado et al., 2018a) is primarily shaped by changes in the population dynamics of malaria vectors, not by the direct impact of environmental fluctuations on malaria infection rates in anopheline vectors. Indeed, we found that environmental variables were uncorrelated with malaria infections in mosquitoes according to our cross-correlation time series analysis.

Finally, the EIR of 0.55 for *An. albimanus* at Ipetí-Guna is one at which transmission is expected to be very efficient, meaning the probability of infection per infective bite is high (Smith et al., 2010), which might explain malaria persistence at Ipetí-Guna and other Guna villages where *An. albimanus* biting behavior and the social and environmental context for malaria transmission are similar (Hurtado et al., 2014; Hurtado et al., 2018a). We also observed *An. albimanus* populations were infected for a period shorter than its period biting humans, as infections were detected only from September to December, peaking in December, three months after a peak in HBR, which occurs in September and lasts from May to December. Thinking on interventions to eliminate malaria from the Gunas, our results suggest that interventions aimed at eliminating the parasite from the human population are the ones most likely to be successful for the social, economic and cultural context of malaria transmission among the Gunas (Hurtado et al., 2014; Hurtado et al., 2018a; Hurtado et al., 2018b). For example, the implementation of Mass Drug Administration (Kaneko, 2010; Kaneko et al., 2000), would be best if deployed during the last half of the dry season, given that March and April is when human landing catches are consistently closer to 0 (Hurtado et al., 2018b). Curtailing infection in humans at that time might reduce positive feedbacks of infection between humans and mosquitoes during the rainy season, as

suggested by a consensus of mathematical models that explicitly monitored infections in human populations subjected to MDA (Brady et al., 2017), which might be critical to keep Guna villages, and Panamá, free of malaria given the delay between mosquito biting humans and mosquitoes being infected with malaria as shown by this study.

Acknowledgements

This research was funded by Ministerio de Economía de la República de Panamá, grant number 9044-024. We thank Sahir Dutary, Susana Isabel Koo, Damaris Bernal, Lorenzo Caceres and Lleysa Pineda for their assistance during field sampling.

References

Beach, R.F., Cordon-Rosales, C., Molina, E., Wirtz, R.A., 1992. Field evaluation of an enzyme-linked immunosorbent assay for estimating the sporozoite rate in *Anopheles albimanus*. Am. J. Trop. Med. Hygiene 47, 478–483.

Beier, J.C., Oster, C.N., Onyango, F.K., Bales, J.D., Sherwood, J.A., Perkins, P.V., Chumo, D.K., Koech, D.V., Whitmire, R.E., Roberts, C.R., Diggs, C.L., Hoffman, S.L., 1994. *Plasmodium falciparum* incidence relative to entomologic inoculation rates at a site proposed for testing malaria vaccines in Western Kenya. Am. J. Trop. Med. Hygiene 50, 529–536.

Beier, J.C., Killeen, G.F., Githure, J.I., 1999. Entomologic inoculation rates and *Plasmodium falciparum* malaria prevalence in Africa. Am. J. Trop. Med. Hygiene 61, 109–113.

Brady, O.J., Slater, H.C., Pemberton-Ross, P., Wenger, E., Maude, R.J., Ghani, A.C., Penny, M.A., Gerardin, J., White, L.J., Chitnis, N., Aguas, R., Hay, S.I., Smith, D.L., Stuckey, E.M., Okiro, E.A., Smith, T.A., Okell, L.C., 2017. Role of mass drug administration in elimination of *Plasmodium falciparum* malaria: a consensus modelling study. Lancet Glob. Health 5, e680–e687.

Breeland, S.G., 1972. Studies on the Ecology of *Anopheles albimanus*. Am. J. Trop. Med. Hygiene 21, 751–754.

Brunsdon, C., Comber, L., 2015. An Introduction to R for Spatial Analysis and Mapping. Sage Publications LTD., London.

Busetto, L., Ranghetti, L., 2016. MODIStsp: an R package for automatic preprocessing of MODIS Land Products time series. Comput. Geosci. 97, 40–48.

Calzada, J.E., Marquez, R., Rigg, C., Victoria, C., De La Cruz, M., Chaves, L.F., Cáceres, L., 2015. Characterization of a recent malaria outbreak in the autonomous indigenous region of Guna Yala, Panamá. Malar. J. 14, 459.

Chaves, L.F., 2016. Globally invasive, withdrawing at home: *Aedes albopictus* and *Aedes japonicus* facing the rise of *Aedes flavopictus*. Int. J. Biometeorol. 60, 1727–1738.

Chaves, L.F., 2017. Climate change and the biology of insect vectors of human pathogens. In: Johnson, S., Jones, H. (Eds.), Invertebrates and Global Climate Change. Wiley, Chichester, UK, pp. 126–147.

Chaves, L.F., Moji, K., 2018. Density dependence, landscape, and weather impacts on aquatic *Aedes japonicus japonicus* (Diptera: Culicidae) abundance along an urban altitudinal gradient. J. Med. Entomol. 55, 329–341.

Chaves, L.F., Imanishi, N., Hoshi, T., 2015. Population dynamics of *Armigeres subalbatus* (Diptera: Culicidae) across a temperate altitudinal gradient. Bull. Entomol. Res. 105, 589–597.

de Zulueta, J., Garrett-Jones, C., 1965. An investigation of the persistence of malaria transmission in Mexico. Am. J. Trop. Med. Hygiene 14, 63–77.

Didan, K., 2015. MOD13Q1: MODIS/Terra Vegetation Indices 16-Day L3 Global 250 m SIN Grid V006. https://doi.org/10.5067/MODIS/MOD13Q1.006]. Last accessed on: October 8, 2018.

Drakeley, C., Schellenberg, D., Kihonda, J., Sousa, C.A., Arez, A.P., Lopes, D., Lines, J., Mshinda, H., Lengeler, C., Schellenberg, J.A., Tanner, M., Alonso, P., 2003. An estimation of the entomological inoculation rate for Ifakara: a semi-urban area in a region of intense malaria transmission in Tanzania. Tropical Med. Int. Health 8, 767–774.

Echeverry, D.F., Deason, N.A., Makuru, V., Davidson, J., Xiao, H., Niedbalski, J., Yu, X., Stevenson, J.C., Bugoro, H., Aparaimo, A., Reuben, H., Cooper, R., Burkot, T.R., Russell, T.L., Collins, F.H., Lobo, N.F., 2017. Fast and robust single PCR for *Plasmodium* sporozoite detection in mosquitoes using the cytochrome oxidase I gene. Malar. J. 16, 230.

Farrington, C., 1992. Estimating prevalence by group testing using generalized linear models. Stat. Med. 11, 1591–1597.

Foley, D.H., Harrison, G., Murphy, J.R., Dowler, M., Rueda, L.M., Wilkerson, R.C., 2012. Mosquito bisection as a variable in estimates of PCR-derived malaria sporozoite rates. Malar. J. 11, 145.

Gorgas, W.C., 1914. Anti-mosquito work at Panama. Proc. R. Soc. Med. 31, 32–40.

Herrera, S., Quiñones, M.L., Quintero, J.P., Corredor, V., Fuller, D.O., Mateus, J.C., Calzada, J.E., Gutierrez, J.B., Llanos, A., Soto, E., Menendez, C., Wu, Y., Alonso, P., Carrasquilla, G., Galinski, M., Beier, J.C., Arévalo-Herrera, M., 2012. Prospects for malaria elimination in non-Amazonian regions of Latin America. Acta Trop. 121, 315–323.

Herrera, S., Ochoa-Orozco, S.A., González, I.J., Peinado, L., Quiñones, M.L., Arévalo-Herrera, M., 2015. Prospects for malaria elimination in mesoamerica and hispaniola. PLoS Negl. Trop. Dis. 9, e0003700.

Herrera-Varela, M., Orjuela, L.I., Peñalver, C., Conn, J.E., Quiñones, M.L., 2014. *Anopheles* species composition explains differences in *Plasmodium* transmission in La Guajira, northern Colombia. Mem. Inst. Oswaldo Cruz 109, 952–956.

Hobbs, J.H., Sexton, J.D., St Jean, Y., Jacques, J.R., 1986. The biting and resting behavior of *Anopheles albimanus* in northern Haiti. J. Am. Mosq. Control Assoc. 2, 150–153.

Hoshi, T., Higa, Y., Chaves, L.F., 2014. *Uranotaenia novobscura ryukyuana* (Diptera: Culicidae) population dynamics are denso-dependent and autonomous from weather fluctuations. Ann. Entomol. Soc. Am. 107, 136–142.

Hoshi, T., Imanishi, N., Moji, K., Chaves, L.F., 2017. Density dependence in a seasonal time series of the bamboo mosquito, *Tripteroides bambusa* (Diptera: Culicidae). Can. Entomol. 149, 338–344.

Hurtado, L.A., Cáceres, L., Chaves, L.F., Calzada, J.E., 2014. When climate change couples social neglect: malaria dynamics in Panamá. Emerg. Microbes Infect. 3, e27.

Hurtado, L.A., Calzada, J.E., Rigg, C.A., Castillo, M., Chaves, L.F., 2018a. Climatic fluctuations and malaria transmission dynamics, prior to elimination, in Guna Yala, República de Panamá. Malar. J. 17, 85.

Hurtado, L.A., Rigg, C.A., Calzada, J.E., Dutary, S., Bernal, D., Koo, S.I., Chaves, L.F., 2018b. Population Dynamics of *Anopheles albimanus* (Diptera: Culicidae) at Ipetí-Guna, a Village in a Region Targeted for Malaria Elimination in Panamá. Insects 9, 164.

Jennings, A.H., 1912. Some problems of mosquito control in the tropics. J. Econ. Entomol. 5, 131–142.

Kaneko, A., 2010. A community-directed strategy for sustainable malaria elimination on islands: Short-term MDA integrated with ITNs and robust surveillance. Acta Trop. 114, 177–183.

Kaneko, A., Taleo, G., Kalkoa, M., Yamar, S., Kobayakawa, T., Björkman, A., 2000. Malaria eradication on islands. Lancet 356, 1560–1564.

Kendall, A.I., 1906a. Malarial infection in certain native villages of the canal zone. JAMA 46, 1151–1154.

Kendall, A.I., 1906b. Malarial infection in certain native villages of the canal zone. JAMA 46, 1266–1273.

Kilama, M., Smith, D.L., Hutchinson, R., Kigozi, R., Yeka, A., Lavoy, G., Kamya, M.R., Staedke, S.G., Donnelly, M.J., Drakeley, C., Greenhouse, B., Dorsey, G., Lindsay, S.W., 2014. Estimating the annual entomological inoculation rate for *Plasmodium falciparum* transmitted by *Anopheles gambiae* s.l. using three sampling methods in three sites in Uganda. Malar. J. 13, 111.

KNMI, 2018. KNMI Climate Explorer. http://climexp.knmi.nl (Last accessed on: October 8, 2018).

Loaiza, J.R., Bermingham, E., Scott, M.E., Rovira, J.R., Conn, J.E., 2008. Species composition and distribution of adult *Anopheles* (Diptera: Culicidae) in Panama. J. Med. Entomol. 45, 841–851.

Macdonald, G., 1952. The analysis of the sporozoite rate. Trop. Dis. Bull. 49, 569–586.

Ministerio de Salud de Panamá, 2011. Manual de Normas y Procedimientos para Malaria República de Panamá. Organización Panamericana de la Salud & Ministerio de Salud de Panamá, Panamá.

Naranjo-Diaz, N., Rosero, D.A., Rua-Uribe, G., Luckhart, S., Correa, M.M., 2013. Abundance, behavior and entomological inoculation rates of anthropophilic anophelines from a primary Colombian malaria endemic area. Parasit. Vectors 6, 61.

Naranjo-Díaz, N., Altamiranda, M., Luckhart, S., Conn, J.E., Correa, M.M., 2014. Malaria vectors in ecologically heterogeneous localities of the colombian pacific region. PLoS One 9, e103769.

NASALPDAAC, 2018. NASA Land Processes Distributed Active Archive Center. https://lpdaac.usgs.gov (Last accessed on: October 8, 2018).

NOAA, 2018a. GHCN_CAMS Gridded 2m Temperature (Land). https://www.esrl.noaa.gov/psd/data/gridded/data.ghcncams.html (Last accessed on: October 8, 2018).

NOAA, 2018b. GPCP Version 2.3 Combined Precipitation Data Set. https://www.esrl.noaa.gov/psd/data/gridded/data.gpcp.html (Last accessed on: October 8, 2018).

Obaldia, N., 2015. Determinants of low socio-economic status and risk of *Plasmodium vivax* malaria infection in Panama (2009–2012): a case–control study. Malar. J. 14, 14.

Obaldia, N., Baro, N.K., Calzada, J.E., Santamaria, A.M., Daniels, R., Wong, W., Chang, H.-H., Hamilton, E.J., Arevalo-Herrera, M., Herrera, S., Wirth, D.F., Hartl, D.L., Marti, M., Volkman, S.K., 2015. Clonal outbreak of *Plasmodium falciparum* infection in Eastern Panama. J. Infect. Dis. 211, 1087–1096.

Patz, J.A., 1998. Predicting key malaria transmission factors, biting and entomological inoculation rates, using modelled soil moisture in Kenya. Tropical Med. Int. Health 3, 818–827.

Patz, J.A., Olson, S.H., 2006. Malaria risk and temperature: influences from global climate change and local land use practices. Proc. Natl. Acad. Sci. U. S. A. 103, 5635–5636.

Pettorelli, N., Vik, J.O., Mysterud, A., Gaillard, J.-M., Tucker, C.J., Stenseth, N.C., 2005. Using the satellite-derived NDVI to assess ecological responses to environmental change. Trends Ecol. Evol. 20, 503–510.

Pinault, L.L., Hunter, F.F., 2012. Characterization of larval habitats of *Anopheles albimanus, Anopheles pseudopunctipennis, Anopheles punctimacula*, and *Anopheles oswaldoi* s.l. populations in lowland and highland Ecuador. J. Vect. Ecol. 37, 124–136.

Póvoa, M.M., Machado, R.L.D., Segura, M.N.O., Vianna, G.M.R., Vasconcelos, A.S., Conn, J.E., 2000. Infectivity of malaria vector mosquitoes: correlation of positivity between ELISA and PCR-ELISA tests. Trans. R. Soc. Trop. Med. Hyg. 94, 106–107.

Rejmankova, E., Savage, H.M., Rejmanek, M., Arredondo-Jimenez, J.I., Roberts, D.R., 1991. Multivariate analysis of relationships between habitats, environmental factors and occurrence of anopheline mosquito larvae *Anopheles albimanus* and *A. pseudopunctipennis* in Southern Chiapas, Mexico. J. Appl. Ecol. 28, 827–841.

Rejmankova, E., Savage, H., Rodriguez, M., Roberts, D., Rejmanek, M., 1992. Aquatic vegetation as a basis for classification of *Anopheles albimanus* Weideman (Diptera: Culicidae) larval habitats. Environ. Entomol. 21, 598–603.

Rejmankova, E., Roberts, D., Harbach, R., Pecor, J., Peyton, E., Manguin, S., Krieg, R., Polanco, J., Legters, L., 1993. Environmental and regional determinants of *Anopheles*

(Diptera: Culicidae) larval distribution in Belize, Central America. Environ. Entomol. 22, 978–992.
Rockett, R.J., Tozer, S.J., Peatey, C., Bialasiewicz, S., Whiley, D.M., Nissen, M.D., Trenholme, K., Mc Carthy, J.S., Sloots, T.P., 2011. A real-time, quantitative PCR method using hydrolysis probes for the monitoring of *Plasmodium falciparum* load in experimentally infected human volunteers. Malar. J. 10, 48.
Rozeboom, L.E., 1938. The Rôle of some Common Anopheline Mosquitoes of Panama in the Transmission of Malaria. Am. J. Trop. Med. Hygiene s1-18, 289–302.
Rozeboom, L.E., 1942. Subspecific variations among neotropical *Anopheles* mosquitoes, and their importance in the transmission of malaria. Am. J. Trop. Med. Hygiene 22, 235–255.
Rubio-Palis, Y., Curtis, C.F., 1992a. Evaluation of different methods of catching anopheline mosquitoes in western Venezuela. J. Am. Mosq. Control Assoc. 8, 261–267.
Rubio-Palis, Y., Curtis, C.F., 1992b. Biting and resting behaviour of anophelines in western Venezuela and implications for control of malaria transmission. Med. Vet. Entomol. 6, 325–334.
Rubio-Palis, Y., Wirtz, R.A., Curtis, C.F., 1992. Malaria entomological inoculation rates in western Venezuela. Acta Trop. 52, 167–174.
Rubio-Palis, Y., Moreno, J.E., Sánchez, V., Estrada, Y., Anaya, W., Bevilacqua, M., Cárdenas, L., Martínez, Á., Medina, D., 2012. Can Mosquito Magnet® substitute for human-landing catches to sample anopheline populations? Mem. Inst. Oswaldo Cruz 107, 546–549.
Shumway, R.H., Stoffer, D.S., 2011. Time Series Analysis and its Applications, 3rd ed. Springer, New York.
Smith, D.L., Drakeley, C.J., Chiyaka, C., Hay, S.I., 2010. A quantitative analysis of transmission efficiency versus intensity for malaria. Nat. Commun. 1, 108.
Snounou, G., Viriyakosol, S., Xin Ping, Z., Jarra, W., Pinheiro, L., do Rosario, V.E., Thaithong, S., Brown, K.N., 1993. High sensitivity of detection of human malaria parasites by the use of nested polymerase chain reaction. Mol. Biochem. Parasitol. 61, 315–320.
Speybroeck, N., Williams, C.J., Lafia, K.B., Devleesschauwer, B., Berkvens, D., 2012. Estimating the prevalence of infections in vector populations using pools of samples. Med. Vet. Entomol. 26, 361–371.
Torres, R., Samudio, R., Carrera, J.-P., Young, J., Márquez, R., Hurtado, L., Weaver, S., Chaves, L.F., Tesh, R., Cáceres, L., 2017. Enzootic mosquito vector species at equine encephalitis transmission foci in the República de Panamá. PLoS One 12, e0185491.
Warren, M., Mason, J., Hobbs, J., 1975. Natural Infections of *Anopheles albimanus* with *Plasmodium* in a Small Malaria Focus*. Am. J. Trop. Med. Hygiene 24, 545–546.
Weathersbee, A.A., 1944. Observations on the Relative Attractiveness of man and Horse for *Anopheles albimanus* Weideman1. Am. J. Trop. Med. Hygiene s1–24, 25–28.
WHO, 1993. Técnicas Entomológicas de Campo para la Lucha Antipalúdica. Parte I, Guía del Alumno. OMS, Ginebra.
WHO, 2018. World Malaria Report 2017. World Health Organization, Geneva.
Wilkerson, R.C., Strickman, D., Litwak, T.R., 1990. Illustrated key to the female anopheline mosquitoes of Central America and Mexico. J. Am. Mosq. Control Assoc. 6, 7–34.
Zetek, J., 1915. Behavior of *Anopheles albimanus* Wiede and *tarsimaculata* Goeldi. Ann. Entomol. Soc. Am. 8, 221–271.
Zimmerman, R.H., 1992. Ecology of malaria vectors in the Americas and future direction. Mem. Inst. Oswaldo Cruz 87, 371–383.